

# Performance Improvement of a Vertical Turbine Pump Accounting for the Solid-Water Two-Phase Flow Conditions

Thomas Alphonse Mbock Singock and Guyh Dituba Ngoma  
*University of Quebec in Abitibi-Témiscamingue, School of Engineering,  
445, Boulevard de l'Université, Rouyn-Noranda, Quebec, J9X 5E4, Canada*

**Keywords:** Vertical Turbine Pump, Two-Phase Flow, ANSYS-CFX.

**Abstract:** A numerical study of the performance of a vertical turbine pump is carried out accounting for the flow of water with solid particles through the pump. For this purpose, the governing equations of two-phase flow are applied and solved using the ANSYS-CFX software. The achieved numerical pump model is validated by comparison with the experimental results when the pump is subjected to clear water to generate the reference pump model. Under two-phase flow, the performance of the reference pump drops drastically. Thus, the results obtained reveal that the morphology of the pump studied favors the obstruction of the hydraulic channels of the diffuser under two-phase flow. Based on this, a geometrical enlargement of hydraulic channels compared to the reference pump model is adopted. The performance under two-phase flow is enhanced while it is observed its slight decrease under single-phase flow.

## 1 INTRODUCTION

The need to move fluids has led to the development of mechanisms exploiting energy transfer. These mechanisms of which pump are exploited in various field and the environment where pumps are in operation may change over time. This is the case of some wells used to ensure the storage tanks for wastewater from mines: the water contains solid particles when its level drops in the tanks.

In the dewatering well, the submersible pump is subjected to a single-phase flow and then gradually to a two-phase flow. With these unusual pumping conditions, when a pump is sized for clear water, it is obvious that a performance problem will quickly arise.

The main challenge in this case is to determine a suitable shape at the pump, allowing it to present close performance when the pump is working under single-phase flow and two-phase flow. To ensure a good efficiency of a pump working under different conditions mentioned, it is necessary to understand the flow inside hydraulic channels and the impact of solid particles on the pump performance. For this fact, some techniques developed in other fields are applied to pumps for two-phase flow applications.

Several numerical and experimental research works have been accomplished on the vertical turbine

pumps in line with improving performance. The aspect on the fluid flow through the pumps, the pump shaft failure and the vibrations acting on the pump shaft have been investigated inter alia by the authors (Birajdar R. S. et al., 2021; Gao Y. et al., 2023; Mohapatra J. N. et al., 2023; Nikumbe A. Y. et al., 2015; Sunil P., 2022; Trivedi J. B. et al., 2016; Xia Y. et al., 2015).

Indeed, the one-way fluid structure interaction (FSI) method has been used for a vertical turbine pump to find out the interaction between the fluid and the structure to determine the vibration displacements (Birajdar R. S. et al., 2021). The authors have demonstrated that this approach can be applied to understand and predict the fluid-induced vibrations in any vertical turbine Pump.

Considering a liquid single-phase flow, a performance study of a multi-stage vertical turbine with different outlet setting angles of the space diffuser has been realized accounting of the high rotating speed of the shaft (Gao Y. et al., 2023). The results obtained reveal that the outlet setting angle of 90° corresponds to an optimal solution.

Moreover, a shaft of a vertical turbine pump has been examined experimentally in terms of failure in tie with the pump operating conditions and the service history of the pump (Mohapatra J. N. et al., 2023). In addition, a modal analysis of a vertical turbine pump

has been done by the authors (Nikumbe A. Y. et al., 2015). The results achieved of the experimental modal analysis and the finite element modal analysis are compared.

The authors (Trivedi J. B. et al., 2016) have analyzed numerically a vertical turbine pump to predict initial design of the pump geometries. They have considered a pump including the impeller and the suction bell. Using a liquid single-phase flow, the streamline and the contours of the pressure and the velocity have been achieved and examined. In the paper (Xia Y. et al., 2015), the authors are described an approach to design and optimize a vertical turbine pump. The sources of loss of efficiency have been identified employing the results of the CFD analysis. According to this approach, the predicted performance of the optimized pump is validated by a physical testing.

In sum, analyzing the previous research works on the vertical turbine pumps, it is observed that the presented results cannot be automatically generalized to all types of vertical turbine pumps. Thus, any new investigation on a vertical turbine pump presents a challenge.

Therefore, in this work, a numerical modeling approach is developed to study in-depth the performance of a vertical turbine pump considering the single-phase flow and the two-phase flow basing on an existing vertical turbine pump. The obtained model of a vertical turbine pump is numerical characterized and validated. Furthermore, the effects of the solid-water two-phase flow, and the diffuser vane number on the pump performance are analyzed.

## 2 MODEL DESCRIPTION AND GOVERNING EQUATIONS

Figure 1 illustrates the main components of the reference vertical turbine pump studied in this research: a suction bell, an impeller, and a diffuser.

To describe the equations of the single-phase flow (liquid flow) and the two-phase flow (solid-liquid two-phase flow) for the flow through a vertical turbine pump as depicted in Figure 1, the assumptions are made. For the liquid single-phase flow, the liquid flow is assumed to be steady-state and three-dimensional; the liquid is considered incompressible; the liquid is a Newtonian liquid; and the liquid thermophysical properties are constant with the temperature.

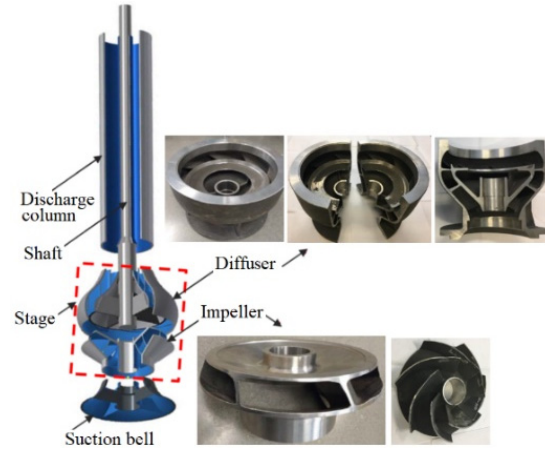


Figure 1: Single-stage pump components (School of Engineering; Mbock Singcock, T. A., 2018).

Moreover, for the solid-liquid two-phase flow, the solid phase consists of dispersed solid particles; the heat transfer and the mass transfer between discrete and continuous phases are negligible; the mixture of phases is heterogeneous; the solid phase is assumed to be uniform spherical particles, and its physical property is unchangeable; the liquid phase is clear water; and the effects of the mass and energy exchange between the solid phase and the liquid phase are negligible.

### 2.1 Single-Phase Flow: Liquid Flow

Accounting for the assumptions for the liquid single-phase flow, the theoretical analysis of the liquid flow in the passages of the impeller, the diffuser vane and the suction bell is based on the continuity and the momentum equations (La Roche-Carrier et al., 2013; ANSYS Inc., 2023). For the three-dimensional liquid flow through these components as shown in Figure 1, the continuity equations are given by:

$$\nabla \cdot \vec{U} = 0 \quad (1)$$

where  $\vec{U} = \vec{U}(u(x,y,z), v(x,y,z), w(x,y,z))$  is the liquid flow velocity vector.

The momentum equations are expressed by:

$$\rho \nabla \cdot (\vec{U} \otimes \vec{U}) = -\nabla p + \mu_{\text{eff}} \nabla \cdot (\nabla \vec{U} + (\nabla \vec{U})^T) + \rho \vec{g} + \vec{S}_M \quad (2)$$

where  $p$  is the pressure;  $\rho$  is the density;  $\mu_{\text{eff}}$  is the effective viscosity accounting for turbulence, it is defined as  $\mu_{\text{eff}} = \mu + \mu_t$ ,  $\mu$  is the dynamic viscosity and  $\mu_t$  is the turbulence viscosity. It is linked to turbulence kinetic energy  $\kappa$  and dissipation  $\varepsilon$ ; and  $\vec{S}_M$  represents the vector Coriolis, the centrifugal effect,

and the drag effect. It is equal to zero for the flow in the stationary components like the diffuser and the suction bell.

More particularly, for the flow in a rotating impeller at a constant angular speed  $\omega$ , the source term can be written as follows:

$$\vec{S}_M = -\rho(2\vec{\omega}x\vec{U} + \vec{\omega}x(\vec{\omega}x\vec{r})) \quad (3)$$

## 2.2 Two-Phase Flow: Solid-Liquid Two-Phase Flow

Related to the solid-liquid two-phase flow through a vertical turbine pump, it is highlighted that the Sommerfeld collision model is applied to consider the collision between particles, and the collision between the solid particles and the wall (ANSYS Inc., 2023; Sommerfeld M., 1982). For that, due to the nature of the mining rocks, the collision is assumed to be fully elastic. To specify the drag, the Schiller Naumann drag model is used supposing that the solid particles are spherical, and the Reynolds number is sufficiently large for inertial effects to dominate viscous effects. Moreover, the dispersed phase zero equation model is applied as the turbulence model. The wear of the pump parts by erosion is not assessed in this study. The volume fraction is given by:

$$\xi_i = \frac{V_i}{V} \quad (4)$$

where  $V_i$  is the volume occupied by the phase  $i$  ( $i = \alpha$  for the liquid phase and  $i = \beta$  for the solid phase); and  $V$  is the volume containing both phases.

According to the particle model, the transfer of the momentum between the solid particles and the water is characterized by the interfacial area density. The interphase contact area can be expressed as follows:

$$A_{\alpha\beta} = \frac{6\xi_\beta}{d_\beta} \quad (5)$$

where  $d_\beta$  is the mean diameter of spherical solid particles and  $\xi_\beta$  is the volume fraction of the solid phase.

To ensure that the area density is not null, the particle model is modified and the Equation (5) becomes:

$$A_{\alpha\beta} = \frac{6\xi_\beta}{d_\beta} \quad (6)$$

where

$$\xi_\beta = \begin{cases} \max(\xi_\beta, \xi_{\min}) & \text{if } \xi_\beta < \xi_{\max} \\ \max\left(\frac{1-\xi_\beta}{1-\xi_{\max}} \xi_{\max}, \xi_{\min}\right) & \text{if } \xi_\beta > \xi_{\max} \end{cases} \quad (7)$$

The values of  $\xi_{\min}$  and  $\xi_{\max}$  in Equation (7) are respectively  $10^{-7}$  and 0.8.

Furthermore, the mass conservation equations of the liquid and solid phases are formulated by:

$$\nabla \cdot (\xi_i \rho_i \vec{U}_i) = 0 \quad (8)$$

where  $i = \alpha$  for the liquid phase and  $i = \beta$  for the solid phase;  $\xi_i$  is the volume fraction of the phase  $i$ ;  $\rho_i$  is the density of the phase  $i$ ; and  $U_i$  is the flow velocity of the phase  $i$ .

Adding the left member of the Equation (8) for the solid phase and the water phase, the Equation (9) is found:

$$\nabla \cdot (\xi_\alpha \rho_\alpha \vec{U}_\alpha) + \nabla \cdot (\xi_\beta \rho_\beta \vec{U}_\beta) = 0 \quad (9)$$

In addition, the volume conservation equation restraint the sum of the volume fraction of both phases to unity at any time, as follows:

$$\xi_\alpha + \xi_\beta = 1 \quad (10)$$

Moreover, the momentum equations for the solid and the liquid phases can be given by:

$$\nabla \cdot [\xi_i (\rho_i \vec{U}_i \otimes \vec{U}_i)] = -\xi_i \nabla p_i + \rho_i \vec{g} + \vec{S}_{Mi} + \nabla \cdot [\xi_i \mu_i (\nabla \vec{U}_i + (\nabla \vec{U}_i)^T)] + \quad (11)$$

where  $p_i$  is the pressure of the phase  $i$ ;  $\mu_i$  is the dynamic viscosity of the phase  $i$ ;  $\vec{S}_{Mi}$  is the source term vector in the context of the two-phase flow. It is formulated as follows:

$$\vec{S}_{Mi} = -\rho_i (2\vec{\omega}x\vec{U}_i + \vec{\omega}x(\vec{\omega}x\vec{r}_i)) \quad (12)$$

Additionally, the characteristics of the solid particles in the liquid that the pump can drain in the mining environment are not always known in advance.

Therefore, considering that the solid particles are dispersed, the diameter, the volume fraction and the specific gravity of a solid particle are varied according to the Table 1.

Table 1: Discrete phase parameters for dispersed solid analysis.

Diameter [mm]	Volume concentration [%]	Specific gravity [-]
1	10	1
2	20	2
3	30	3

### 3 DESIGN PARAMETERS OF THE COMPONENTS OF A VERTICAL TURBINE PUMP

The developed numerical approach to design the impeller, the diffuser and the suction bell of a vertical turbine pump is based on an existing physical pump and a process of trial and error using the references (Dicmas J. L., 1987; La Roche-Carrier et al., 2013; Peng W. W., 2008; Stepanoff A. J., 1957). This approach accounts for the operating conditions of the pump which is the mining environment. Thus, Figure 2 shows the steps from the design point to the numerical characterization of the vertical turbine pump.

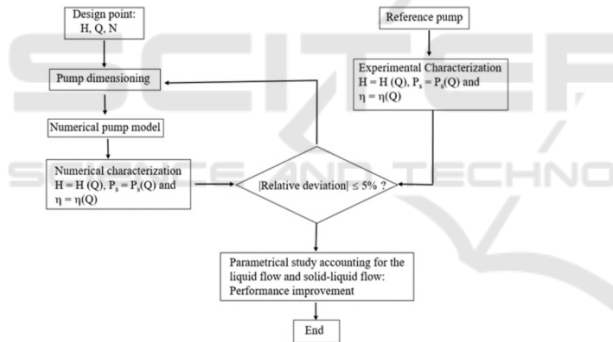


Figure 2: Steps of the numerical characterization of the vertical turbine pump.

Furthermore, the parameters of the impeller, the suction bell, and the diffuser are depicted in Figure 3. To achieve the numerical model of the vertical turbine pump, the design point used is described by a flow rate of 0.11 m<sup>3</sup>/s, a pump head of 35 m and a rotating speed of 1785 rpm. The pump type is determined calculating the specific speed which is given by:

$$N_s = \frac{NQ^{1/2}}{H^{3/4}} \quad (13)$$

where Q is the flow rate, H is the pump head, and N is the rotating speed.

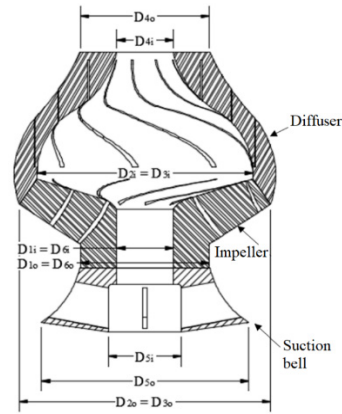


Figure 3: Suction bell, impeller, and diffuser.

The corresponding dimensionless specific speed can be expressed as follows:

$$N_{ad} = \frac{\omega Q^{1/2}}{(gH)^{3/4}} \quad (14)$$

where  $\omega$  is the angular speed.

According to the value of  $N_s$ , the reference vertical pump under study is Francis's type (Peng W. W., 2008). This geometry is classified between radial and axial pumps. Physically, this reflects the fact that the flow inside the Francis-type pump is semi-axial.

Moreover, the following assumptions are formulated for the dimensioning of the impeller, the diffuser, and the suction bell: the inlet flow in the impeller is considered without circumferential component; the outlet blade angle of the pump impeller is considered as constant; and the ratio of the inner and the outer radius of the impeller is kept constant.

### 4 ELEMENT MESH, VERTICAL TURBINE PUMP MODELING AND BOUNDARY

Equations (1), (2), (9) and (11) resulting from the mathematical modeling are solved numerically while accounting for the boundary conditions and the turbulence model by means of the ANSYS-CFX code to obtain the distributions of the liquid flow velocity and the pressure for the liquid single-phase flow and the solid-liquid two-phase flow. In the cases examined involving the pump stage, the boundary conditions are formulated as follows: the static pressure is given at the stage inlet, while the flow rate is specified at the stage outlet. The frozen rotor condition is applied for the impeller-diffuser interface

and the suction bell-impeller interface. In sum, Figure 4 shows the element mesh and the boundary conditions for the pump model.

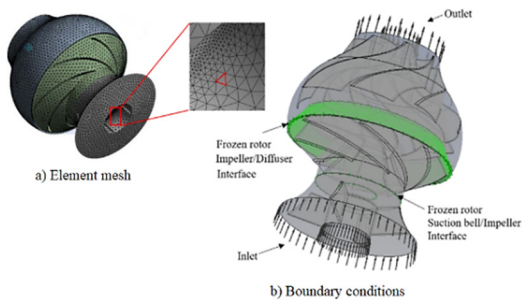


Figure 4: Element mesh and pump boundary conditions.

## 5 RESULTS AND DISCUSSION

The used properties of the 17-4PH steel (impeller, diffuser, and shaft) and the water in this study are indicated in Tables 2 and 3.

Table 2: Properties of the 17-4PH steel.

Young's modulus [Pa]	$1.96 \times 10^{11}$
Poisson ratio	0.3
Compressibility module [Pa]	$1.63 \times 10^{11}$
Shear modulus [Pa]	$7.53 \times 10^{10}$
Resistance coefficient [Pa]	$9.2 \times 10^8$
Ductility coefficient [Pa]	$10^9$
Yield strength [Pa]	$7.93 \times 10^8$
Ultimate tensile strength [Pa]	$1.103 \times 10^9$
Density [kg/m <sup>3</sup> ]	7750.4

Table 3: Properties of water in 25 °C.

Density [kg/m <sup>3</sup> ]	Kinematic viscosity [m <sup>2</sup> /s]
997	$0.884 \times 10^{-6}$

Furthermore, the main reference data for the impeller, diffuser and suction bell are indicated in Table 4.

Table 4: Reference data for the impeller, the diffuser and the suction bell.

Impeller	$D_h = 70$ mm; $D_1 = 160$ mm; $D_{1m} = 123$ mm; $D_2 = 310.6$ mm; $D_{2m} = 288.64$ mm; $D_{2i} = 288.64$ mm; $b_1 = 64$ mm; $b_2 = 38$ mm; $\beta_1 = 19^\circ$ ; $\beta_2 = 27.5^\circ$ ; and $Z = 7$ .
Diffuser	$D_3 = 310.6$ mm; $D_{3i} = 266.68$ mm; $D_4 = 160$ mm; $l_c = 190.9$ mm; $b_3 = 45.12$ mm; $\beta_3 = 30^\circ$ ; $\beta_4 = 90^\circ$ ; and $Z_d = 8$ .
Suction bell	$D_5 = 256.17$ mm; $D_6 = 160$ mm; $L_c = 68, 45$ mm; $R_c = 115.36$ mm; and $Z_c = 4$ .

As regards the numerical simulations performed, three cases are analyzed for the performance assessment of the considered vertical turbine pump: a) the characterization and the validation of the numerical model using water single-phase flow; b) the effect of the solid-water two-phase flow; and c) the effect of the diffuser vane number.

### 5.1 Characterization and Validation of the Numerical Model

To characterize the developed numerical pump model in terms of head, brake horsepower and efficiency using the water single-phase flow, the flow rate range from 170.25 m<sup>3</sup>/h to 520.75 m<sup>3</sup>/h are selected keeping the other parameters constant. Figure 5 represents the pump head, the brake horsepower and the efficiency as a function of the flow rate. From this figure, it can be seen the trend of the performance curves of the vertical turbine pump. The head decreases with increasing flow rate. The brake horsepower raises with the augmentation of the flow rate, whereas the efficiency raises till the best efficiency point (BEP), then it decreases with growing flow rate. At the BEP, the flow rate is 397.25 m<sup>3</sup>/h, the head is 35.52 m, the brake horsepower is 50.73 kW and the efficiency is 78.54 %. Furthermore, the numerical results are compared with the experimental results to validate the numerical pump model. A very good agreement is achieved for the curves of the head and the efficiency as depicted in Figures 6 and 7 respectively. The corresponding relative gaps in absolute value of the comparison results as a function of the flow rate are shown in Figure 8. Thus, the validated numerical model is designated as a reference model for the analysis of performance improvement accounting for the two-phase flow of water and solid particles.

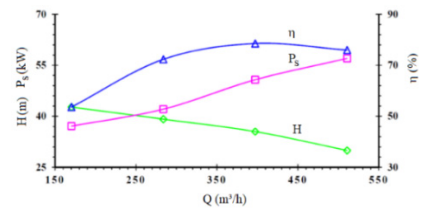


Figure 5: Head, brake horsepower and efficiency versus flow rate.

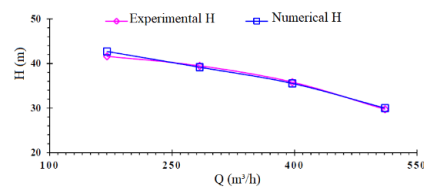


Figure 6: Head comparison.

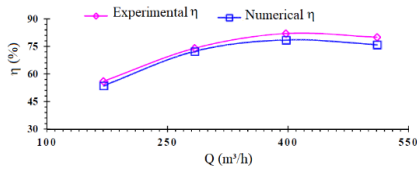


Figure 7: Pump efficiency comparison.

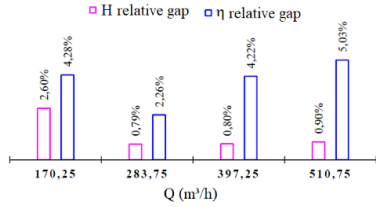


Figure 8: Relative gap between experimental and numerical results.

### 5.2 Effect of the Solid-Water Two-Phase Flow

To analyze the effect of the solid-water two-phase flow on the pump head, the brake horsepower and the efficiency, the reference model is used considering the two-phase flow of water and solid discrete particles. The applied values for the volume fraction of solid particles, the solid particles diameter and the specific gravity of the solid particles are 10 %, 1 mm and 2, respectively. In addition, the flow rate range from 170.25 m<sup>3</sup>/h to 520.75 m<sup>3</sup>/h are selected. Figure 9 illustrates the pump head, the brake horsepower and the efficiency as a function of the flow rate for water flow and the solid-water two-phase flow. From there, it can be seen that the head and the efficiency for the water flow are better than these for the solid-water two-phase flow, whereas the brake horsepower is almost identical for both flow types. The drops in the pump head and the efficiency represent the impact of the solid particles on the flow field in the pump.

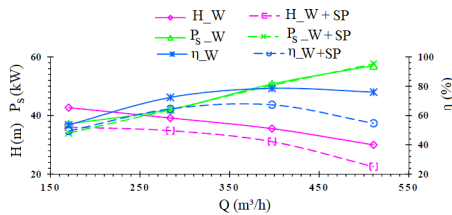


Figure 9: Head and efficiency versus flow rate: single-phase (W) and two-phase (W+SP) flow.

### 5.3 Effect of the Diffuser Vane Number

To investigate the effect of the diffuser vane number on the pump performance accounting for the water

single-phase flow (SPF) and the solid-water two-phase flow (TFP), the vertical turbine pump model with 7 diffuser vanes is selected while holding the other parameters constant for the flow rate from 280.5 m<sup>3</sup>/h to 510 m<sup>3</sup>/h. This pump model is designated as modified model to distinguish it from the reference model that has 8 diffuser vanes. Figs. 10-12 show the pump head, the brake horsepower and the efficiency as a function of the flow rate with the diffuser vane number as a parameter. From Figure 10, it is observed that the pump head for the solid-water two-phase flow with the modified model is greater than that with the reference model. Moreover, the gap between the pump heads for the water flow with the reference and the modified models is lower than the gap for the solid-water two-phase flow with the reference and modified models. In addition, Figure 11 shows that the brake horsepower for the solid-water two-phase flow with the modified model is slightly higher than the brake horsepower of all other cases. Relating to the pump efficiency, Figure 12 illustrates that the efficiency for the solid-water two-phase flow with the modified model is between the efficiencies for the water single-phase flow and the solid-water two-phase flow with the reference model. Thus, comparing the efficiencies of the reference and the modified models accounting for the solid-water two-phase flow, it can be mentioned that the efficiency is better for the modified model. This can show that the modified model is at this level of assessment, best suited to withstand the variations required by the transition from water flow to solid-water two-phase flow without any functional or installation modification.

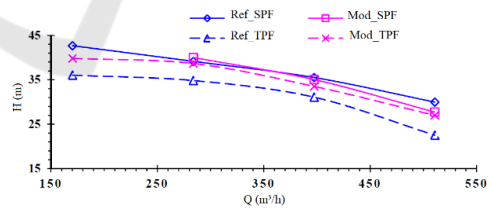


Figure 10: Head versus flow rate: reference and modified models.

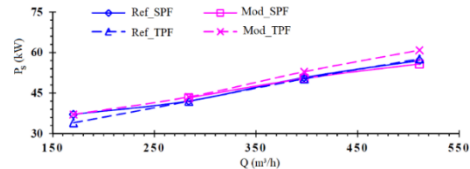


Figure 11: Brake horsepower versus flow rate: reference and modified models.

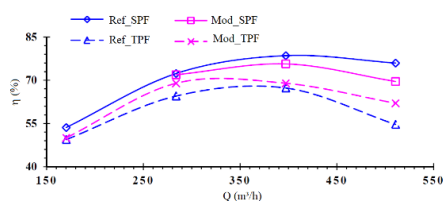


Figure 12: Efficiency versus flow rate: reference and modified models.

In sum, it is to highlight that the use of 7 diffuser vanes in the modified pump model leads to a widening of the diffuser channels of 13.8 % as indicated in Figure 13.

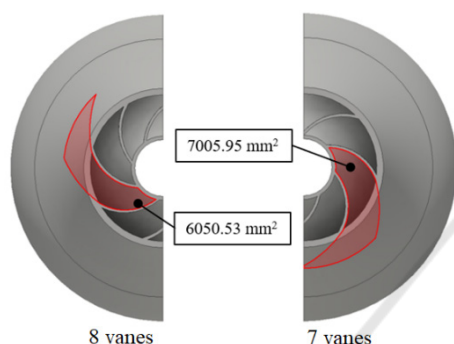


Figure 13: Modified diffuser channels.

## 6 CONCLUSIONS

This study deals with the design and the numerical characterization of a vertical turbine pump in the context of the performance enhancement. Based on the design point, the numerical model of a vertical turbine pump of Francis type is developed. By means of the ANSYS CFX code, the pump head, the brake horsepower and the efficiency are determined in different operating conditions using the water single-phase flow to obtain the reference model after validation. A very good agreement is achieved comparing the numerical results from the reference model and the experimental results. Then, simulations are accomplished with the reference model considering the solid-water two-phase flow. It is observed that the pump head and the efficiency for the water two-phase flow are lower than those for the water single-phase flow, whereas the brake horsepower is remained almost unchanged. Thus, to improve the performance of the reference model in the case of the solid-water two-phase flow, the diffuser with 7 vanes is used keeping the impeller blade number of 7 to obtain the modified model. The comparison of the numerical results between the

reference model and the modified model revealed an improvement of the head and the efficiency for the modified model. Further research work is planned to analyze the effects of the induced forces and stresses on the vertical turbine pump performance in the mining environment.

## ACKNOWLEDGEMENTS

The authors are grateful to the Technosub Inc., Industrial pumps manufacturing and distribution in Quebec (Canada) and the Turbomachinery laboratory of the Engineering School of the University of Quebec in Abitibi-Témiscamingue.

## REFERENCES

- ANSYS Inc., ANSYS CFX-Solver Theory Guide Release 2023 R1. Canonsburg, PA, USA, 2023.
- Birajdar R. S., Keste A. A., and Gawande S. H. (2021). Critical Hydraulic Eccentricity Estimation in Vertical Turbine Pump Impeller to Control Vibration, *International Journal of Rotating Machinery*.
- Dicmas J. L. (1987). *Vertical turbine, mixed flow, and propeller pumps*, McGraw-Hill Book Company New York.
- Gao Y., Cao W., Zhang Y., Cao G. and Zhao X. (2023). Investigation of high-speed deep well pump performance with different outlet setting angle of space diffuser, *Frontiers in Energy Research*.
- La Roche-Carrier N., Dituba Ngoma G., and Ghie W. (2013). Numerical investigation of a first stage of a multistage centrifugal pump: impeller, diffuser with return vanes, and casing. *ISRN Mechanical Engineering*, Vol. 2013, Article ID 578072, 15 pages.
- Lazarkiewicz, S., TROSLANSKI, A. T. (1965). *Impeller pumps*. Pergamon Press Ltd., Headington Hill Hall, Oxford.
- Mbock Singock, T. A. (2018). *Conception et caractérisation numérique d'une pompe à turbine verticale de grande capacité*. Université du Québec en Abitibi-Témiscamingue.
- Mohapatra J. N., Gujare R. R., Dabir S. K., Sah R. (2023). Failure Analysis of Vertical Turbine Pump Shaft, *Journal of Failure Analysis and Prevention (JFAP)*.
- Nikumbe A. Y., Tamboli V. G., Wagh H. S. (2015). Modal Analysis of Vertical Turbine Pump, *International Advanced Research Journal in Science, Engineering and Technology*.
- Peng W. W. (2008). *Fundamentals of turbomachinery*, John Wiley & Sons, California.
- School of Engineering, Turbomachinery laboratory (E-216), University of Quebec in Abitibi-Témiscamingue (UQAT), www.uqat.ca.

- Sommerfeld M. (1982). Modelling of Particle-Wall Collisions in Confined Gas-Particle Flows, *International Journal of Multiphase Flow*, 18(6), pp. 905-926.
- Stepanoff A. J. (1957), *Centrifugal and Axial Flow Pumps, Theory, Design, and Application*, John Wiley & Sons, New York.
- Sunil P. (2022). Testing of Mixed Flow Vertical Turbine Pump, *International research journal of engineering and technology (IRJET)*.
- Trivedi J. B., Trivedi J., Chauhan V. (2016). Hydraulic Analysis of Vertical Turbine Pump, *INROADS- An International Journal of Jaipur National University*.
- Xia Y., Maddox G., S. Lowry and Ding H. (2015), Design and Optimization of a Vertical Turbine Pump, *Proceedings of the ASME/JSME/KSME. Joint Fluids Engineering Conference. Volume 1: Symposia. Seoul, South Korea. V001T33A008. ASME. DOI: 10.1115/AJKFluids2015-33233.*

